A Numerical Study of the Influence of Advective Accelerations in an Idealized, Low-Latitude, Planetary Boundary Layer

LARRY J. MAHRT[1,2]

Dept. of Meteorology, University of Wisconsin, Madison 53706

(Manuscript received 16 March 1972, in revised form 27 July 1972)

ABSTRACT

Steady, longitudinally invariant, barotropic, boundary layer flow is numerically studied at low latitudes where advective accelerations may be large and the Coriolis parameter is small. Flow is generated by specifying the pressure gradient field independent of the flow.

It is found that as the flow approaches the equator, advective terms associated with the large latitudinal variation of the Coriolis parameter become important. As the flow crosses the equator, advective accelerations may become important to the extent that the boundary layer downstream from the equator is radically different from the Ekman boundary layer. Compared to Ekman flow, the wind vector may rotate with height in the opposite direction, and the boundary layer depth may be considerably thinner and less dependent on latitude. The cross-isobar flow of this advective boundary layer is deeper and may be stronger, so that spatial transitions between this boundary layer and a quasi-Ekman boundary layer can produce significant vertical motion.

1. Introduction

The dynamics of low-level flow at low latitudes is not well understood because of the simultaneous importance of momentum transport by both turbulent and larger scale motions. Flow at very low latitudes, especially cross-equatorial flow, cannot adjust to the local Coriolis parameter which varies rapidly with latitude and reverses sign at the equator. As a result advective and time accelerations will likely be important compared to the small Coriolis terms.

Theoretical and empirical studies of rotating viscous boundary layers in the presence of advective terms (e.g., Greenspan, 1968; Kuo, 1971) indicate that in regions of small rotation, the boundary depth is large but finite, and rotation of the wind vector with height is small. Pushistov (1970) numerically solved the special case of steady, zonally invariant, equatorially symmetric, boundary layer flow. It appeared that advections became more important as the flow approached the equator. However, isolation of the influence of advections was not possible since he chose special baroclinic pressure fields (where the advecting velocity did not reverse sign with height).

Calculations from observations by Janota (1971) indicate that momentum advections are important mainly equatorward from the Intertropical Convergence Zone (ITCZ). The low-level wind vector generally rotates with height in the Ekman direction poleward from the ITCZ (Gray, 1968; Janota, 1971) and rotates in either direction equatorward from the ITCZ (Robitaille and Zipser, 1970; Janota, 1971). These observations suggest that an Ekman-like balance of forces is often strongly violated equatorward from the ITCZ.

The present study will numerically examine the influence of momentum advections associated with the strong latitudinal variation of the Coriolis parameter at low latitudes. It will be shown that these advections alone can upset the geostrophic-Ekman balance of forces to the extent that the resulting flow is radically different from Ekman flow.

2. Formulation

To emphasize the effect of these advections, zonally invariant, steady barotropic flow is assumed. A height independent eddy diffusivity ($5\ m^2\ sec^{-1}$) and a "no-slip" lower boundary condition are chosen so that the effects of momentum advection terms are easily isolated by comparisons with the known Ekman (1905) solution (no advections). Of course, in actuality, eddy diffusivity is a function of both space and time, especially in the presence of low-level convective clouds and the strong thermal stratification of the trade inversion.

The above assumptions make quantitative comparisons with actual atmospheric data somewhat precarious. On the other hand, inclusion of time accelerations,

[1] This study was carried out when the author was a Ph.D. candidate. He was subsequently associated with the National Center for Atmospheric Research, Boulder, Colo., which is sponsored by the National Science Foundation.

[2] Present affiliation: Department of Atmospheric Sciences, Oregon State University, Corvallis.

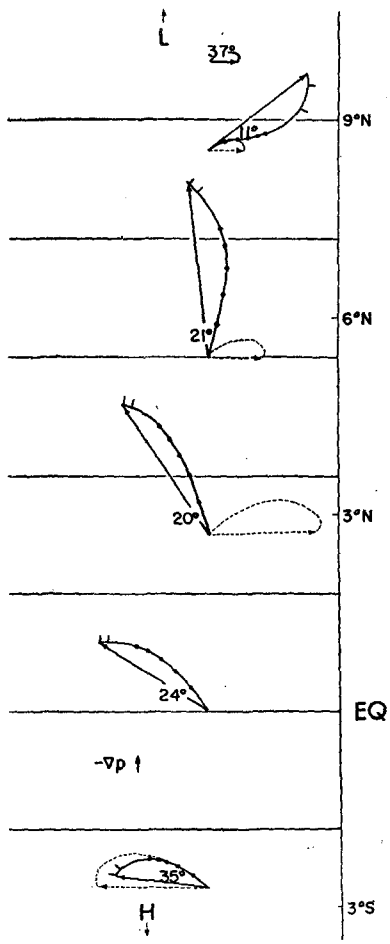

FIG. 1. Steady boundary layer wind hodographs (solid spirals) and surface pressure fields for a latitudinally independent, meridional pressure gradient of -4×10^{-5} m^2 sec^{-1}. Solid thin lines denote surface isobars at increments of 0.1 mb. Wind hodographs (solid lines) are shown for various latitudes where dots indicate elevations 200, 400, . . . , 1000 m, and hash marks indicate elevations of 2000 and 3000 m. The hypothetical Ekman hodographs as interpreted by the grid system (dashed lines, not defined at the equator) are also shown. The solid and dashed vectors denote, respectively, the computed and Ekman wind at 4000 m. The angle between the 200 m and 4000 m wind is also indicated. Actual latitudinal boundaries of the numerical experiment are 8S and 12N.

baroclinity, zonal variations, and a more sophisticated representation of turbulent transports would prevent isolation of the influence of advective accelerations. It is hoped that the fundamental effects of advective accelerations, as conveniently revealed by this simplified study, will also be appropriate to actual atmospheric flows. Various pressure fields will be specified independently of the flow to emphasize specific dynamical features. Pressure adjustments forced by the flow and a somewhat more realistic parameterization of turbulent momentum transports are included in Mahrt (1972b).

The appropriate time-dependent equations of motion on an equatorial β-plane and the steady incompressible continuity equation are written as:

$$\frac{\partial u}{\partial t}+v\frac{\partial u}{\partial y}+w\frac{\partial u}{\partial z}=\beta yv-\alpha\frac{\partial p}{\partial x}+K\frac{\partial^2 u}{\partial z^2}, \tag{1}$$

$$\frac{\partial v}{\partial t}+v\frac{\partial v}{\partial y}+w\frac{\partial v}{\partial z}=-\beta yu-\alpha\frac{\partial p}{\partial y}+K\frac{\partial^2 v}{\partial z^2}, \tag{2}$$

$$\frac{\partial v}{\partial y}+\frac{\partial w}{\partial z}=0, \tag{3}$$

where α is the constant specific volume, p pressure, β the Rossby parameter, K the eddy diffusivity, and other symbols are defined in the usual sense. To preserve zonal invariance of the flow, $\alpha(\partial p/\partial x)$ must be independent of both x and y, while $\alpha(\partial p/\partial y)$ can be specified to be any arbitrary function of y.

The differencing of time derivatives employs forward differencing while the advective terms employ upstream differencing. The differencing of the diffusion term is

$$\frac{\partial^2 v}{\partial z^2}=(v^{n}_{j+1}-2v^{n+1}_{j}+v^{n}_{j-1})/\Delta z^2$$

where superscripts are the time step indicator, subscripts the vertical grid index, and Δz is the vertical grid increment. This scheme is advantageous because it is always stable in the equations of motion (Mahrt, 1972a) and the resulting system of equations can be evaluated explicitly. Numerical experiments, where the exact analytical solution is known, indicate that this particular scheme is preferable over other difference schemes of this type, because its "inconsistent truncation errors" behave more favorably in the equations of motion. However, its preference over the alternating Saul'ev scheme is slight. The calculation of vertical motion and streamfunction ($\partial\psi/\partial z=v$) employs centered differencing and vertically staggered grid points. The continuity equation at its lowest grid level assumes linear extrapolation of $\partial v/\partial y$ to the surface. Vertical motion at main grid levels is computed with simple averaging.

Finite-differenced equations are evaluated at grid points at vertical increments of 200 m and horizontal increments of 50 km. The model contains 20 levels in the vertical. The latitudinal boundaries vary with experiment and are given in the figure legends. Zero vertical shear of the horizontal wind is specified at 4000 m while zero horizontal shear of the horizontal wind is specified at side boundaries. The Ekman solution is specified as an initial flow state. The differenced equations of motion are iterated for a real time of 16 days with time increments of 500 sec.

3. Latitudinal flow variations

In the first three numerical experiments, flow is generated by latitudinally independent pressure gra-

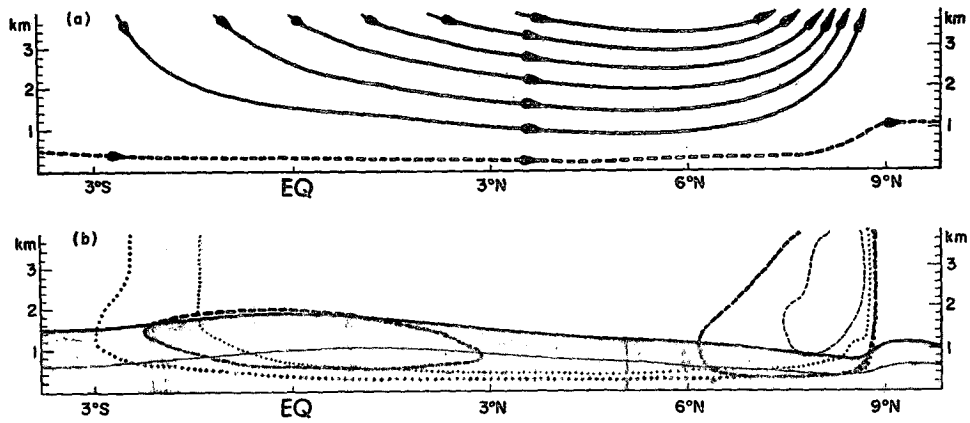

FIG. 2. Steady streamlines and relative "forces" for the case of constant meridional pressure gradient: (a), streamlines in the y-z plane in increments of 4×10^3 m^2 sec^{-1} where the dashed line is the 2×10^2 m^2 sec^{-1} streamline; and (b), isopleths of relative "forces" (the vector magnitude of the term divided by the vector magnitude of the largest term in the equations of motion at its particular grid point). Values of 0.50 (thin lines) and 0.20 (thick lines) for the diffusion term (solid lines), the vertical advection term (dashed lines), and the horizontal advection term (dotted lines) are shown. Shading denotes the region where the relative diffusion term exceeds 0.20.

dient fields. In this manner, latitudinal variations of the flow response are initiated solely by latitudinal variations of the Coriolis parameter.

In the first experiment (Figs. 1–3), the pressure gradient is directed in the meridional direction. As quasi-Ekman flow approaches the equator, momentum advections associated with latitudinal variations of the Ekman depth, $(2K/\beta y)^{\frac{1}{2}}$, and geostrophic wind become important. In fact, the Ekman solution indicates that these advections, relative to the pressure gradient term, are $O(U_g/\beta y^2)$. Advection terms in the steady state are smaller than those calculated from the Ekman solution, since the advections tend to reduce spatial flow variations. Fig. 2b shows that the steady-state horizontal advections are most important in the middle portion of the boundary layer where the advecting velocity (which in this case is also the cross-isobar component) is largest.

Figs. 1–2 indicate that the effect of these advections is to decrease the rotation of the wind vector with height and to decrease the boundary depth, especially at the equator (where the Ekman depth is infinite). The level below which the momentum diffusion term at a given grid point exceeds 20% of the maximum term at that grid point is used as an indication of boundary layer depth. The above effects can also be qualitatively predicted by estimating advections from the Ekman solution.

As the flow crosses the equator, the zonal wind component suddenly opposes the direction of the zonal Ekman wind (which reverses sign at the equator). The flow is then accelerated rapidly toward lower pressure,

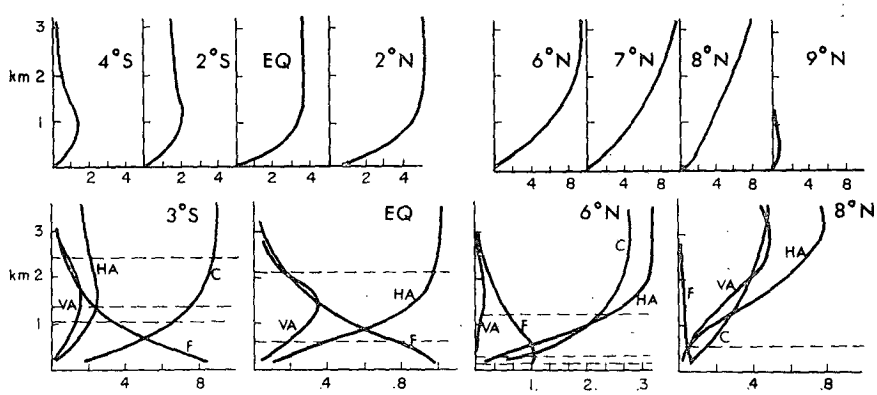

FIG. 3. Vertical profiles of meridional flow (m sec^{-1}) and magnitudes of forces and momentum advections for the case of constant meridional pressure gradient. The top row of figures illustrates the evolution of the meridional flow across the two flow transition regions. The lower row of figures shows vertical profiles of the vector magnitude of the diffusion (F), vertical advection (VA), horizontal advection (HA), and Coriolis (C) terms which are all normalized with respect to the magnitude of the constant horizontal pressure gradient force. Horizontal dashed lines separate regions defined by different combinations of terms whose relative importance exceeds 0.20.

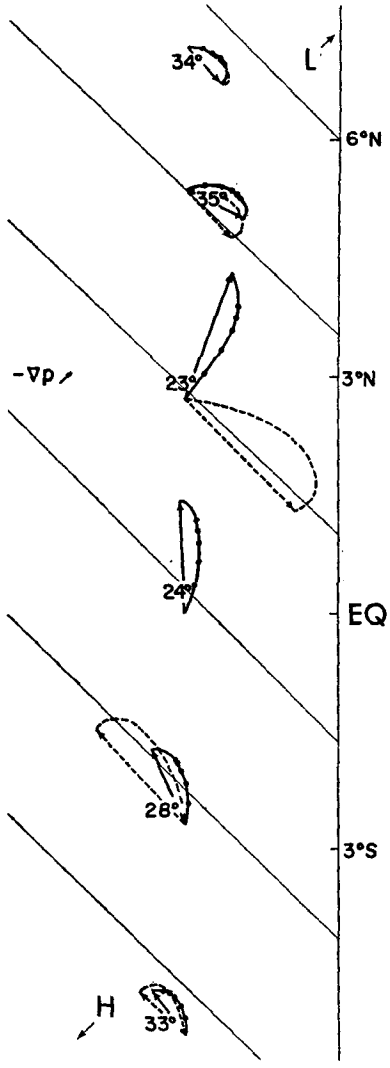

FIG. 4. Boundary layer wind and surface pressure fields for $\partial p/\partial x = \partial p/\partial y = -2.84 \times 10^{-5}$ m^2 sec^{-1}. Actual boundaries of numerical experiment are at 10S and 10N. See Fig. 1 for further explanation.

eventually achieving Ekman equilibrium further downstream. The flow solution at large heights, where the horizontal pressure gradient is "balanced" by Coriolis and horizontal advective accelerations, is easily obtained for any continuous zonally, invariant, meridional pressure gradient distribution (see Appendix). This solution indicates that the cross-isobar flow speed is dependent on the square root of the pressure gradient and a function of the upstream ageostrophic flow. Varying the pressure gradient magnitude in different experiments verifies this tendency.

The boundary layer downstream from the equator, where advective accelerations are large, will be referred to as the "advective boundary layer." Since pressure adjustments are not allowed in the experiments, the details of the flow will not be emphasized. However, the basic differences between the advective boundary layer and Ekman flow are significant, since they appear to occur for a wide spectrum of pressure fields generating cross-equatorial flow. In particular, the wind vector downstream from the equator rotates with height in the opposite direction of Ekman rotation. This difference reflects the influence of opposite hemisphere characteristics through advective terms. Analyses of data from the Line Islands (4S–6N, 155W–171W) by Robitaille and Zipser (1970) indicate that the low-level wind vector statistically rotates in the Ekman direction with equatorward flow but rotates in the opposite direction when the flow is poleward (perhaps originating in the opposite hemisphere). The frequency of counter-Ekman rotation for a given wind direction decreased with increasing latitude. Estoque (1971) constructed a mean wind profile at Christmas Island (2N, 157W), which included all wind cases regardless of direction. His analyses, which neglected time and advective accelerations, indicated that counter-Ekman rotation might also be explained in terms of baroclinity.

Fig. 3 shows that cross-isobar flow of the advective boundary layer increases with height and reaches a maximum at the top of the boundary layer (in contrast to Ekman flow where it reaches a maximum in the boundary layer and vanishes aloft). Consequently, if the horizontal pressure gradient does not vary rapidly with latitude, subsidence is produced at the equator in the transition from a quasi-Ekman boundary layer to an advective boundary layer. In this experiment, strong subsidence is produced at the equator (Fig. 2a), since cross-isobar flow is accelerated at all levels. Although comparisons with the actual atmosphere require extreme caution, it is perhaps noteworthy that mean satellite cloud pictures (Kornfield and Hasler, 1969) indicate that the Pacific equator tends to be consistently cloud free. Zipser (1970) has suggested that adiabatic warming compensates for the observed radiational cooling near the equator in the Line Islands region (Cox and Hastenrath, 1970). In the present experiment, subsidence is produced solely by a latitudinal flow transition since the horizontal pressure gradient is independent of latitude.

Conversely, in the transition from advective boundary layer flow to quasi-Ekman flow further downstream, the dramatic decrease in depth and strength of the cross-isobar flow produces strong rising motion. This transition is narrow and intense since flow deceleration results in rising motion and upward advection of lower momentum which in turn causes further deceleration. The detailed horizontal structure of the transition zone is beyond the horizontal resolution of this study. It is noteworthy, however, that the strong vertical motion is again produced solely by a flow transition. Janota (1971) observed that the ITCZ statistically separates two different flows, where advective accelerations are important mainly in the flow equatorward from the ITCZ. He also observed that the meridional flow was deeper equatorward from the ITCZ. A case study of

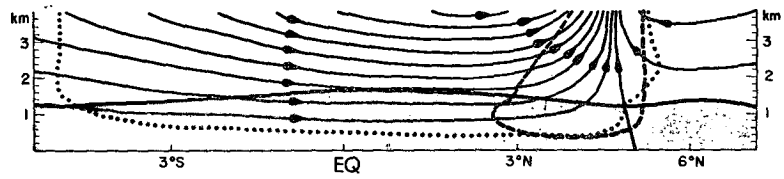

FIG. 5. Streamlines (increments of 2×10^3 m^2 sec^{-1}) and 0.20 relative "force" isopleths for $\partial p/\partial x=\partial p/\partial y=-2.84\times10^{-5}$ m^2 sec^{-1}. See Fig. 2 for further explanation.

streamline analyses (Fujita *et al.*, 1969) indicates that cross-equatorial flow contributes to the convergence of zonally-elongated cloud systems in the ITCZ. One could then conjecture that cross-equatorial flow and a resulting deep layer of cross-isobar flow may be a component in the maintenance of statistical mass convergence in the ITCZ.

Fig. 3 shows that the magnitude of advective accelerations increases with height in the advective boundary layer. As a result the transition to quasi-Ekman flow occurs first in the lowest levels. In other words, the horizontal adjustment scale of the flow to the local Coriolis parameter and pressure gradient increases with height. In fact, Fig. 1 shows that at one point in the transition region the wind vector rotates in the Ekman direction in lower layers and in the opposite direction at higher levels. Janota (1971) found statistical evidence for this phenomena for poleward boundary layer flow between the ITCZ and the equator.

Further upstream in the advective boundary layer, counter-Ekman rotation is small in the lower layers and increases with height. Even though advective accelerations are small in the lowest levels, the wind vector is still not quasi-Ekman due to frictional coupling with flow at higher levels. Of course the vertical scaling of the above height dependencies is exaggerated in the numerical experiment, since the "no-slip" boundary condition does not account for the strong vertical wind shear in the surface layer. The horizontal adjustment scale may also be exaggerated since pressure adjustments are not allowed.

4. Boundary layer depth

The depth of the advective boundary layer, based on the relative local importance of the diffusion term (Fig. 2b), decreases slowly with latitude as the advective term (generally the largest term away from the surface) increases with latitude. In the transition to quasi-Ekman flow, this boundary layer depth increases rapidly as the advective term decreases rapidly. Based on the absolute values of the diffusion term, the boundary depth is more independent of latitude. In terms of the level where the wind reaches a certain percentage of its free atmosphere value or where vertical shears decrease to certain value, the boundary layer depth decreases downstream from the equator where the flow accelerates. This boundary layer depth then increases and achieves a local maximum in the region where the flow is decelerated and upward advections of lower momentum are important. This measure of boundary layer depth is often observed to increase (decrease) in decelerated (accelerated) regions (e.g., Schlichting, 1968, pp. 626–655). The confining influence of subsidence on boundary layer depth can be easily seen in the case of equatorially symmetric flow at the equator where the boundary layer depth is inversely proportional to subsidence strength (Mahrt, 1972a).

Varying the magnitude of eddy diffusivity in various numerical experiments indicates that at a given latitude the depth of the advective boundary layer tends to be proportional to $K^{\frac{1}{2}}$, as would be expected from theory of accelerated viscous flows. Using a height-dependent eddy viscosity (where K is constant up to 500 m and decreases linearly to 10% of this value at 1700 m, above which it is again constant) and applying a geophysical lower boundary condition ($\partial V/\partial z=k_0V$, $k_0=1.5\times10^{-3}$ m^{-1}) reduces the magnitude and latitudinal variations of the boundary layer depth.

5. Other pressure fields

The basic flow regimes for the case of constant meridional pressure gradient can also be generated by a wide variety of other pressure fields which produce cross-equatorial flow. For example, consider the flow generated by rotating the pressure fields of the previous experiment 45° clockwise (Figs. 4 and 5). Differences between this flow and the flow of the previous experiment stem mainly from the different orientation of the upstream quasi-Ekman flows. Equatorward flow now occurs in both hemispheres and is stronger in one hemisphere. Thus, a convergence of two flows is produced in the hemisphere with the weaker equatorward flow. It must be emphasized that again a convergence zone is produced solely by the latitudinal variation of the flow response to a latitudinally independent pressure gradient. The advecting (meridional) velocity in the upstream quasi-Ekman flow is now stronger since the geostrophic wind contains a component in the meridional direction. Consequently, the importance of advective terms and modification of the Ekman flow are important at higher latitudes.

When the pressure field of the first experiment is rotated 45° counterclockwise, a divergence of two flows is produced close to the equator. The meridional flow

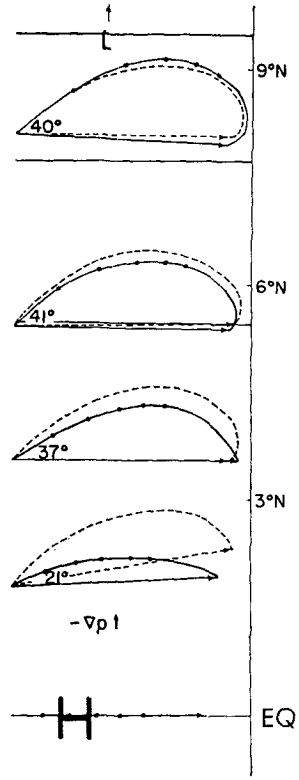

Fig. 6. Boundary layer wind and surface pressure fields for constant westerly geostrophic wind with non-zero flow (quasi-geostrophic aloft) at the equator. Actual boundaries of numerical experiment are 0° latitude and 15° latitude. Isobars are shown in increments of 0.5 mb. See Fig. 1 for further explanation.

and horizontal advections are then small at the equator so that the zonal pressure gradient and downward advections of higher momentum are essentially balanced by momentum diffusion. This results in very strong zonal flow.

Pressure fields "even symmetric" with respect to the equator, $p(y)=p(-y)$, can produce equatorially "odd symmetric" meridional flow, $v(y)=-v(-y)$. Since meridional flow vanishes at the equator, the various flow regimes, which occurred in cross-equatorial flow cases, no longer necessarily occur. Pressure gradient forces directed equatorward or toward the east produce an impingement of two flows at the equator on a horizontal scale beyond the resolution of this study. Pressure gradient forces directed poleward or toward the west produce a divergence of two flows at the equator. Consider the pressure field corresponding to a latitudinally independent, westerly geostrophic wind (high pressure at the equator). Two zonal wind solutions are possible at the equator: the trivial solution $u(z)=0$, and a zonal wind profile which represents a balance between downward advection of higher momentum and momentum diffusion. Figs. 6–9 show that the flows produced in these two cases are quite different. In the case of nonvanishing flow at the equator, the flow aloft is quasi-geostrophic[3] and advections reach a maximum in the boundary layer interior. The flow gradually becomes quasi-Ekman at a relatively low latitude. In contrast, zero flow at the equator causes a large in-

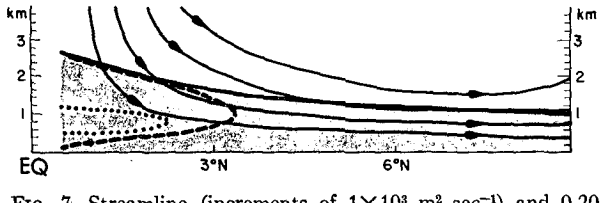

Fig. 7. Streamline (increments of 1×10^3 m^2 sec^{-1}) and 0.20 relative "force" isopleths for constant westerly geostrophic wind with non-zero flow at the equator. See Fig. 2 for further explanation.

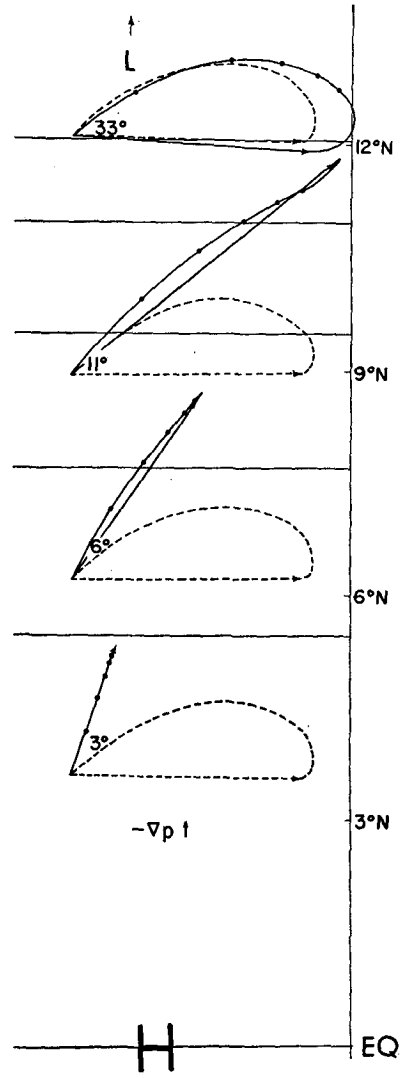

Fig. 8. Boundary layer wind and surface pressure fields for the case of constant westerly geostrophic wind with zero flow at the equator. Actual boundaries of numerical experiment are 0° latitude and 15° latitude. Isobars are shown in increments of 0.5 mb. See Fig. 1 for further explanation.

[3] The zonal flow at the equator, which is initially specified to be the Ekman solution at ¼° latitude, changes very slowly in time.

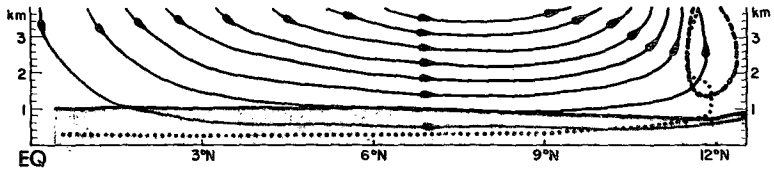

FIG. 9. Streamlines (increments of 4×10^3 m^2 sec^{-1}) and 0.20 relative "force" isopleths for constant westerly geostrophic wind with zero flow at the equator. See Fig. 2 for further explanation.

balance of forces aloft, producing an extensive region where advective accelerations are important. In fact, the exact solution for flow above the boundary layer indicates that the distance required for adjustment to geostrophic equilibrium is dependent on the square root of the upstream ageostrophic wind (see Appendix). Flow in the boundary layer is now much less Ekman-like due mostly to coupling with the highly ageostrophic flow aloft. These differences indicate that large accelerations aloft can induce significant accelerations in the boundary layer.

6. Conclusions

Flow crossing the equator or unbalanced forces near the equator can produce a flow downstream where advective accelerations are large. The boundary layer flow in this region may be radically different from Ekman flow in that the wind vector may rotate with height in the opposite direction, the boundary layer depth is relatively thin and varies slowly with latitude even near the equator, and cross-isobar flow increases with height throughout the boundary layer. As a partial consequence of the latter feature, large vertical motions can be produced in transitions between this boundary layer and quasi-Ekman flow. Since wind speeds and horizontal advections increase with height in the advective boundary layer, the horizontal distance required for adjustment to Ekman flow also increases with height.

As mentioned earlier, some of the basic features of the above simplified flow appear to have possible atmospheric counterparts or provide partial explanation of certain observed phenomena. Because of the much greater complexity of the atmosphere and the lack of boundary layer observations at low latitudes, the validity of such comparisons is not known at this time. Pressure adjustments forced by large vertical motions at the boundary layer transitions is likely to be an important effect. Free atmosphere pressure adjustments forced by low latitude boundary layer flow is examined in Mahrt (1972b).

Acknowledgments. The author wishes to sincerely thank his advisor, Prof. John Young, who made many helpful suggestions at all stages of the research. Thanks are also extended to Profs. David Houghton and Heinz Lettau for their helpful discussions and to Lois Gries who typed the manuscript. This research was supported by NOAA Grant E-230-68-G and NSF Grant GA 30676.

APPENDIX

Width of the Adjustment Region

The equations of motion at large elevations, where $\partial V/\partial z$ and $\partial^2 V/\partial z^2$ vanish, reduce to

$$v\frac{\partial u}{\partial y}=\beta y v, \tag{A1}$$

$$v\frac{\partial v}{\partial y}=-\beta y u-\alpha\frac{\partial p}{\partial y}. \tag{A2}$$

These equations possess two possible solutions: the geostrophic solution in which case $u=U_g$ and $v=0$, and the constant angular momentum solution

$$u=u_o+\beta(y^2-y_o^2)/2,$$
$$v=v(v_o,u_o,y_o,y)\neq 0,$$

where the "o" subscript refers to upstream boundary conditions. Substituting the latter solution for u into (A2) and integrating from y_o to y,

$$v^2=v_o^2+2G(y)-2\alpha(p-p_o), \tag{A3}$$

where

$$G(y)\equiv-\beta[-(u_o y_o^2/2+\beta y_o^4/8)+y^2(u_o/2-\beta y_o^2/4)+y^4\beta/8].$$

If the pressure gradient term [the third term on the right-hand side of (A3)] is negligible, then inertial flow results (e.g., Winn-Nielsen, 1970). Mörth (1963) solved (A2) in the special case where $-\alpha\partial p/\partial y=A=$ constant, *viz.*,

$$v^2=v_o^2+2G(y)+2A(y-y_o).$$

It is instructive to look at the above equations in terms of geostrophic wind, even though the flow may be highly ageostrophic. In the case of a pressure field corresponding to a constant geostrophic wind, (A3) becomes

$$v^2=v_o^2+2G(y)+\beta U_g(y^2-y_o^2). \tag{A4}$$

Of interest is the latitude y^* at which the meridional flow vanishes, which is where the wind first becomes locally geostrophic. The distance between this latitude and the initial latitude defines the latitudinal extent

of the influence of the initial ageostrophic wind (i.e., the width of the adjustment region where horizontal advections are important).

At y^* where $v(y^*)=0$, (A4) becomes

$$0=v_o^2-2\beta[-u_o y_o^2/2+\beta y_o^4/8+y^{*2}(u_o/2-\beta y_o^2/4)+y^{*4}\beta/8]+\beta U_g(y^{*2}-y_o^2),$$

which is a quadratic equation in y^{*2}. Defining

$$u_a=u_o-U_g \quad \text{and} \quad |\mathbf{V}_a|=(u_a^2+v_o^2)^{\frac{1}{2}},$$

and solving the quadratic equation yields

$$y^{*2}-y_o^2=-2u_a/\beta\pm 2|\mathbf{V}_a|/\beta, \tag{A5}$$

where the sign of the second term on the right-hand side is positive (negative) for northerly (southerly) flow in the Northern Hemisphere and vice versa in the Southern Hemisphere. Eq. (A5) implies that the width of the adjustment region is proportional to the square root of the ageostrophic wind at the equator. Factoring the left-hand side

$$y^*-y_o=(-u_a\pm|\mathbf{V}_a|)/\beta\bar{y},$$
$$\bar{y}=(y^*+y_o)/2.$$

Thus, the width of the adjustment region is also inversely proportional to latitude.

REFERENCES

Cox, S. K., and S. Hastenrath, 1970: Radiation measurements over the equatorial central Pacific. *Mon. Wea. Rev.*, **98**, 823–832.

Ekman, V. W., 1905: On the influence of the Earth's rotation on ocean currents. *Arkiv. Mat. Astron. Fysik*, **2**.

Estoque, Mariano, 1971: The planetary boundary layer wind over Christmas Island. *Mon. Wea. Rev.*, **99**, 193–201.

Fujita, T., K. Watanabe and T. Izawa, 1969: Formation and structure of equatorial anticyclones caused by large-scale cross-equatorial flows determined by ATS-I photographs. *J. Atmos. Sci.*, **8**, 669–693.

Gray, William, 1968: Global view of the origin of tropical disturbances and storms. *Mon. Wea. Rev.*, **96**, 669–693.

Greenspan, H. P., 1968: *The Theory of Rotating Fluids.* Cambridge University Press, 328 pp.

Janota, Paul, 1971: An empirical study of the planetary boundary layer in the vicinity of the Intertropical Convergence Zone. Ph.D. thesis, Dept. of Meteorology, M.I.T., Cambridge, Mass., 279 pp.

Kuo, H. L., 1971: Axisymmetric flows in the boundary layer of a maintained vortex. *J. Atmos. Sci.*, **28**, 20–41.

Kornfield, J., and A. F. Hasler, 1969: A photographic summary of the earth's cloud cover for the year 1967. *J. Appl. Meteor.*, **8**, 687–700.

Mahrt, L. J., 1972a: A numerical study of advective effects on boundary layer flow at low latitudes. *Studies of the Atmosphere Using Space Probings*, Ann. Rept. 1971, Space Science and Engineering Center, University of Wisconsin, Madison, 1–147.

——, 1972b: A numerical study of coupling between the boundary layer and free atmosphere in an accelerated low-latitude flow. *J. Atmos. Sci.*, **29**, 1485–1495.

Mörth, H. T., 1963: Fourth seminar on tropical meteorology in Africa. East African Meteorology Dept., Nairobi.

Pushistov, P., 1970: The planetary atmospheric boundary layer in the equatorial region. *Izv. Atmos. Oceanic Phys.*, **6**, 556–564.

Robitaille, F. E., and E. J. Zipser, 1970: Atmospheric boundary layer circulations equatorward of the Intertropical Convergence Zone. *Preprints of Papers, Symp. on Tropical Meteorology*, Honolulu, Amer. Meteor. Soc., C IV-1 to C IV-6.

Schlichting, H., 1968: *Boundary-Layer Theory.* New York, McGraw Hill, 747 pp.

Winn-Nielsen, A. C., 1970: On inertial flow. Rept. No. 1, Institute for Teoretisk Meteorologi, Copenhagen.

Zipser, E. J., 1970: The Line Islands Experiment, its place in tropical meteorology, and the rise of the fourth school of thought. *Bull. Amer. Meteor. Soc.*, **51**, 1136–1146.